Express Polymer Letters Vol.17, No.5 (2023) 471–486
Available online at www.expresspolymlett.com
https://doi.org/10.3144/expresspolymlett.2023.35

Research article

Enhancement of performance in flax/epoxy composites by developing interfacial adhesion using graphene oxide

Abdolmajid Alipour[*]*, Richard Lin, Krishnan Jayaraman*

Centre for Advanced Composite Materials, Department of Mechanical Engineering, The University of Auckland, Auckland, New Zealand

Received 14 September 2022; accepted in revised form 1 December 2022

Abstract. Graphene oxide (GO) at different contents, ranging from 0 to 0.5 wt%, was exploited to develop the interfacial adhesion between matrix and fiber in flax/epoxy composites. A proposed mechanism, which was substantiated by Fourier transform infrared spectroscopy, demonstrated that GO, thanks to possessing oxygen-containing functional groups, acted as a coupling agent between epoxy matrix and flax fiber. As a result of the developed interfacial bonding between composite constituents, significant improvements in tensile strength (68%) and flexural strength (65%) of composites up to 0.3 wt% were recorded. According to X-ray diffraction (XRD) and transmission electron microscopy (TEM) observations, all nanocomposites formed an exfoliated structure. Microscopic observations depicted a substantial decline in the total crack lengths of composites and also the rate of cracks formed at the interface of fiber and matrix. It was also found that thanks to the developed interfacial adhesion between epoxy matrix and flax fiber, major defects responsible for composite premature failure did substantially reduce. In low-velocity impact test, resultant nanocomposites showed enhanced peak loads and damage tolerance owing to a strong interfacial adhesion developed by GO presence. Scanning electron microscopy (SEM) images of the impact-fractured surface of nanocomposites showed the risk mitigation of catastrophic damages, with the inclusion of GO, due to the efficient fiber adherence to the matrix.

Keywords: *nanocomposites, reinforcements, graphene oxide, interfacial strength, mechanical properties*

1. Introduction

Natural fibers such as flax are regarded as an environmentally friendly classification of reinforcement for composite materials which possess excellent stiffness, weight ratio and damping properties [1]. Despite being more expensive than glass fiber, the rate of nonrenewable energy for the production of flax fiber is significantly less than that required for glass fiber [2, 3]. It should also be noticed that in terms of environmental friendliness and human toxicity, flax fiber is superior to synthetic counterparts like glass and carbon fiber [4].

Epoxy matrix is an ideal thermoset for manufacturing large constructions where a combination of low cost and high durability is required. In addition, the chemical structure of epoxy contains hydroxyl and epoxide groups which can create a chemical bonding with free hydroxyl groups of flax fiber that then improves load transfer between fiber and matrix [5]. The good performance of flax/epoxy composites mainly stems from the original properties of flax fiber. Containing nearly 60–80% of cellulose and having a low cellulose microfibril angle, flax fiber possesses the highest strength (800–1000 MPa) among all natural counterparts [6]. More importantly, compared to other bast fibers like hemp and jute, once flax fiber is retted, it can produce more individual elementary fibers contributing to the higher surface area, which is desirable for load transfer in composites [7]. Nonetheless, the ultimate performance

[*]Corresponding author, e-mail: aali352@aucklanduni.ac.nz

of flax/epoxy composites is still less than glass fiber/epoxy ones [8].

In order to improve the performance of flax/epoxy composites, one promising measure is to strengthen the interfacial adhesion between fiber and matrix. These include but are not restricted to developing coupling agents, removing waxy materials from fiber surface, and matrix modification [9–13]. The aforementioned modification methods have been reported to be effective in enhancing the inter-laminar mechanical properties but at a high cost and complexity. However, of all, matrix modification is regarded as an easy and cost-effective process that does not compromise the mechanical and structural properties of composites [14]. Reportedly, the enhancement in mechanical properties is highly dependent on the interface-to-volume ratio and filler size [14]. As a result, nanofillers, thanks to their exclusive characteristics such as high aspect ratio, do play a pivotal role in the matrix modification of fiber-reinforced composites. The modification combines the effects of mechanical interlocking, chemical bonding, and local stiffness of the polymer matrix [14]. In this regard, modification has been implemented by using nanoparticles such as carbon nanotubes (CNTs), TiO_2, nanoclay, and graphene nanoplatelets (GNPs) [15].

Quite recently, GNPs filled composites have been at the center of attention due to the outstanding thermal, electrical, and mechanical properties they bring about [16–18]. In pursuance of obtaining optimum mechanical properties in fiber-reinforced composites, some problematic issues, such as dispersion uniformity of nanoparticles and surface modification of GNPs for a desirable interaction with polymer matrix should be obviated. The strong van der Waals forces in GNPs, which promote the agglomeration of nanosheets, hinder the formation of an exfoliated structure in the resultant composite and consequently bring about a minimal enhancement in mechanical properties [12]. In order to surmount this challenge, other derivatives of GNPs, like graphene oxide (GO), have been exploited so that the affinity between nanoparticles and polymer matrix increases [13]. GO is a derivative form of GNPs encompassing oxygen-rich functional groups, such as carboxyl, epoxide, and hydroxide, which are capable of creating hydrogen and covalent bonding [18]. Albeit GO possesses inferior mechanical properties compared to GNPs, GO-filled fiber-reinforced composites show much better load transfer from matrix to fiber [9, 13]. In this regard, an increase of 66, 72, and 25%, respectively in flexural strength, flexural modulus, and interlaminar shear strength (ILSS) of carbon fiber epoxy composites reinforced with 0.3 wt% of GO was reported [13]. In another study [19], an 89% increase in interfacial shear strength of GO-reinforced jute/epoxy composites was observed. Sarker *et al*. [19] also achieved a 96% improvement in tensile strength of GO-coated jute fiber reinforced epoxy composites. Pereira *et al*. [20] investigated the effect of GO incorporation (0.2 wt%) into either matrix or fiber on the impact toughness of ramie fiber/epoxy composites. While GO addition into fiber showed no significant improvement when it was added to the matrix, the impact toughness improved by 21%. The aforementioned substantial improvements, along with the limited investigations conducted in the field of natural fiber composites reinforced with GO highlight the requisition of further research to examine the potential of GO-nanomodification in high-demand bast fiber-based composites like flax/epoxy for achieving higher performance.

Hence, in this study, GO was incorporated into the polymer matrix with a solvent method which then impregnated flax fiber. The creation of bonding between composite constituents was examined by Fourier transform infrared spectroscopy (FTIR), and a mechanism for the chemical reaction was proposed. Then, following assessing the nanostructure in resultant samples by X-ray diffraction (XRD) and transmission electron microscopy (TEM), the developed interfacial strength between matrix and fiber, due to GO incorporation, was evaluated by both macroscopic and microscopic methods. Finally, the low-velocity impact-related properties were investigated, and the effects of developed interfacial strength on these properties in flax/epoxy nanocomposites were extensively discussed.

2. Materials and characterisation details

2.1. Materials

Diglycidylether of bisphenol A (DGEBA) epoxy resin (viscosity at 25 °C: 430 cP, density at 25 °C: 1180 kg/m^3, pot life at 25 °C (40–50 min), molecular weight: 340 g/mol), 105 West System and polyamine curing agent (209 extra slow hardener), were supplied by Adhesive Technologies Ltd., New Zealand. Graphene oxide, which was synthesized according to Hummer's method in a study [21], was applied in this research to reinforce flax/epoxy composites.

Linen flax woven fabric (2×2 twill weave, density: 1428 kg/m^3, areal weight: 145 g/m^2, wrap direction ends: 25.1 end/cm, weft direction ends: 24 end/cm) was obtained from Libero, Belgium.

2.2. Nanocomposites preparation

In the first step, the designated amounts of GO (0, 0.1, 0.2, 0.3, 0.4, and 0.5 wt%) were added to the epoxy. For this purpose, first, GO was mixed with ethanol. Next, the mixture was mixed by a magnetic stirrer for 45 minutes at room temperature. Then, epoxy resin was added to the solution and mixed by a shear mixer for 90 minutes at the rotor speed of 2000 rpm. Subsequently, to get rid of the residual ethanol, the mixture was heated for 8 hours at the temperature of 80 °C under shear mixing with a low rotor speed (200 rpm). Further, the hardener was added, manually stirred for 1–2 minutes, and the resultant mixture was degassed in the vacuum chamber at room temperature for 5 minutes.

To manufacture flax/epoxy nanocomposites, hand-lay-up method was used. Following spraying the aluminum mould with a release agent, flax fabrics were placed between steel plates. Next, fabric layers were impregnated with GO/epoxy mixture and stacked to each other. To disperse resin more uniformly and remove any trapped bubble, each fabric layer was rolled with a roller. Subsequently, the prepared laminates were cured under a pressure of 0.7 MPa at room temperature for 72 hrs. Finally, the cured laminates were post-cured based on the manufacturer's datasheet to remove the residual stress. To keep consistency in results, fiber volume fraction in all prepared laminates was kept 30%, calculated according to ASTM D2584, as (Equation (1)):

$$V_f = \frac{\rho_m \cdot W_f}{\rho_m \cdot W_f + \rho_f \cdot W_m} \quad (1)$$

where V_f symbolizes fiber volume fraction, W_f weight of fibers, W_m weight of matrix, ρ_f density of fibers, and ρ_m density of matrix. The labels of FE, FEGO1, FEGO2, FEGO3, FEGO4, and FEGO5 represent flax/epoxy composites reinforced with 0, 0.1, 0.2, 0.3, 0.4, and 0.5 wt% of GO, respectively.

2.3. Characterisation

FTIR spectra of samples were recorded from the wavenumber of 4000 to 500 cm^{-1} using a Nicloet FTIR spectrophotometer (USA). Then, FTIR data were collected and processed using OMNIC spectroscopy software. X-ray diffraction of flax/epoxy nanocomposites was recorded with a D2 Phaser Bruker diffractometer (USA) by using a Cu K_α radiation source (the wavelength λ = 1.5406 Å, voltage of 45 kV, electric current of 300 mA and the scanning rate of 5°/min). The range of 2θ scanning was between 10 to 60°. The nanostructures in flax/epoxy nanocomposites were viewed using a Philips CM 200 TEM (USA). To prepare samples for this particular analysis, the specimens were cut by a microtome, hot-pressed between two glass substrates and collected onto copper grids. During microtoming, the knife was oscillated along the direction of the knife edge with an oscillation frequency of 12 kHz, knife forward speed of <0.2 mm/s, a bevel angle of 45–55°, and a clearance angle of 10–15°. The oscillation was produced by a piezo-driven with a sine wave (~30 V peak-to-peak). The morphology of impact or tensile fractured surfaces of nanocomposites was viewed using a scanning electron microscope (SEM, FEI Quanta 200F, USA) following coating with platinum. Tensile properties of nanocomposites were measured by Instron 5567 (UK) based on ASTM D 3039, using samples of dimensions (250×25×2.8 mm). The tensile test was carried out using a crosshead speed of 2 mm/min and a gauge length of 50 mm. Flexural properties of prepared nanocomposites were also determined according to ASTM D790 using Instron 4465 machine (UK). The specimens for this particular analysis were rectangular (70×12.7 mm), while the crosshead speed and the length of the supporting span were set according to the thickness of the sample, as indicated in the relevant standard. The interlaminar shear strength (ILSS) of nanocomposites was measured according to ASTM D2344 (UK). In this study, the samples with the dimensions of (15.3×5.1×2.8 mm) were placed at the center of a three-point fixture in an Instron 4465 testing machine (UK). The span length was 10.18 mm, while the crosshead speed was set at 1 mm/min. In all mechanical analyses, at least five samples were tested, and the average results were reported. To measure the rate of crack density, tensile fracture surfaces of nanocomposites, in square shapes, were cut, encapsulated in a cylindrical container of epoxy resin, and kept for at least 12 hrs so that the resin cured and got rigid. Then, the surfaces of cylindrical resin containers were polished through six levels ending with the grade of 1 μm. Subsequently, the polished surfaces were examined using OLYMPUS BX-60 (UK) microscope.

The impact properties of nanocomposites were measured using a fully instrumented drop weight impact tester (Model IM 10T-201TS, Imatek, UK) based on ASTM D7136 using a hemispherical impactor with a diameter of 16 mm. This impactor was used to obtain the energy-time and force-deflection histories of the composite specimens (150×100×2.6 mm). The mass of the whole impacting system, including the impactor nose, force transducer, and crosshead, was 9.745 kg. All samples were exposed to the impact force of 18.5±1.2 J. In this study, a TA Instruments Q800 (USA) was used for the dynamic mechanical analysis (DMA) which was implemented in a single cantilever. Samples of dimensions 35×2 mm under a tension mode, at the frequency of 1 Hz, the dynamic strain of 0.1% in the temperature from 20 to 200 °C and the heating rate of 3 °C/min.

3. Results and discussion

3.1. Fourier transform infrared spectroscopy (FTIR)

The existence of different functional groups on the surface of GO was evaluated with FTIR, as seen in Figure 1. Results indicate that GO contains oxygenated groups on its surface because of the characteristics peak at 3445 cm^{-1}, which is ascribed to the stretching vibrations of carbonyl (C=O) and carboxyl (COOH) groups. Moreover, the peaks at 1639, 1463, and 1127 cm^{-1} are ascribed to the stretching vibration of C=C, C–OH, and C–O, respectively. The peaks pertaining to the stretching vibrations of the epoxy ring also appear in 1264 and 1028 cm^{-1} [13].

Additionally, flax/epoxy composites reinforced with and without GO were characterized by FTIR. In FTIR spectra of plain flax/epoxy composites, the peaks at 2871 and 2928 cm^{-1} are respectively related to the vibrations of asymmetric and symmetric CH_2 and CH_3 groups [13]. The peaks at 1235 and 820 cm^{-1}, respectively correspond to the presence of asymmetric stretching mode and symmetric stretching mode of C–O bond of vinyl ether. More importantly, the carbonyl peak position in flax/epoxy/GO nanocomposites is observed at 1651 cm^{-1}, while this peak in GO spectrum appears at 1735 cm^{-1}. The carbonyl peak of GO also shifts to a lower frequency which is ascribed to the formation of H-bond with OH groups of the epoxy polymer. The alteration in the position of the mentioned peak is due to the formation of H-bonding between epoxy and GO, which consequently lowers the bond strength of the carbonyl bond, leading to shifting in the peak [13]. Moreover, the wide band that appeared between 3400 and 3000 cm^{-1} is due to the stretching vibration of OH groups in flax fiber. After the incorporation of GO, a significant decrease in the intensity of this peak is observed, which is ascribed to the stretching of O–H hydroxyl groups substantiating that the addition of GO to the polymer matrix efficiently creates crosslinking with the O–H group on the surface of both cellulose chain and matrix [13]. Figure 2 also schematically shows the proposed reaction in which how GO influences flax/epoxy composites.

3.2. Morphology of flax/epoxy/GO nanocomposites

3.2.1 X-ray diffraction (XRD)

X-ray diffraction (XRD) is a reliable technique to determine the degree of intercalation and exfoliation in the composites. XRD spectra of graphene oxide, plain flax/epoxy, and different nanocomposites are

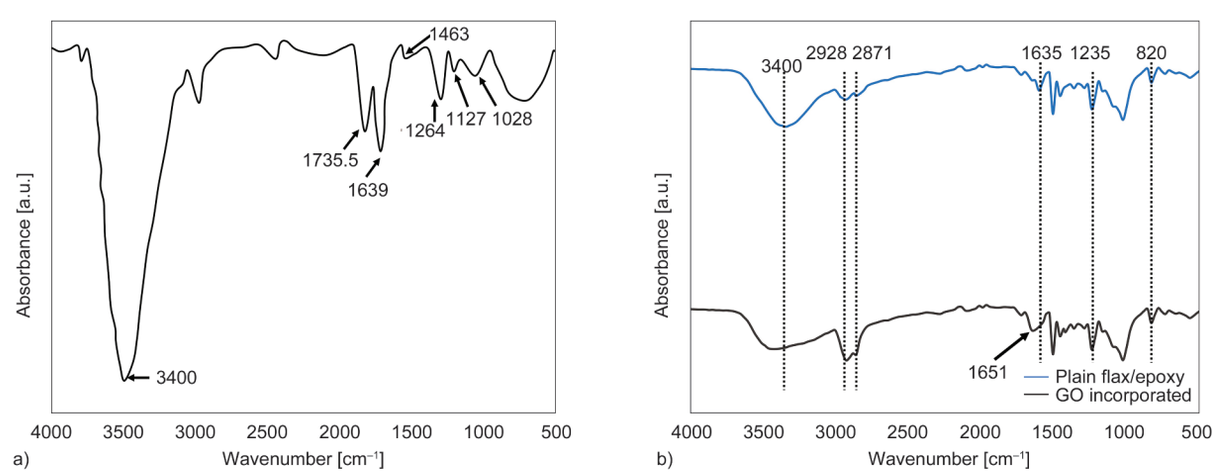

Figure 1. FTIR plot of a) GO b) plain, NaOH treated and 0.3 wt% GO-incorporated flax/epoxy composite.

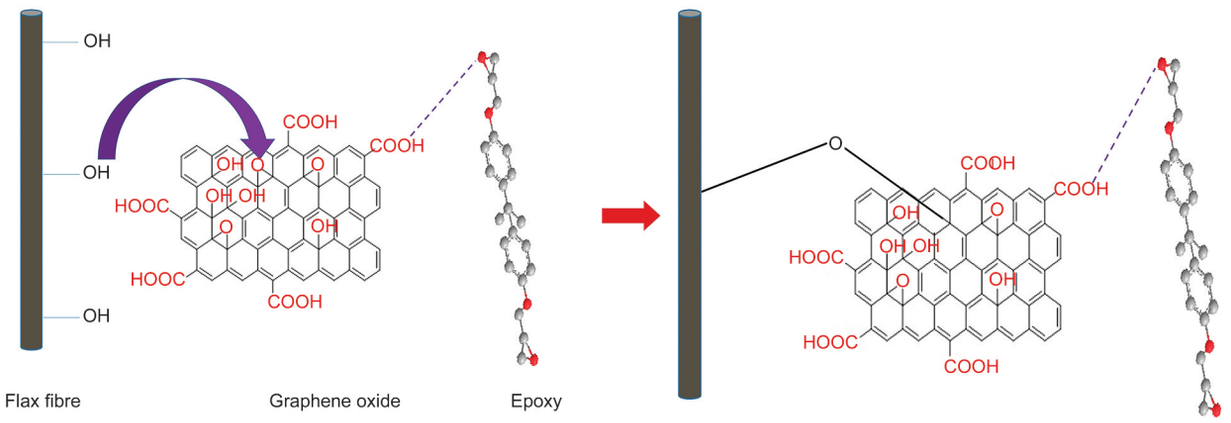

Figure 2. Proposed mechanism of GO influencing flax/epoxy composite.

illustrated in Figure 3. As seen, a peak at 2θ =10.18° appears relating to the (002) plane of GO [13]. According to Bragg's law of diffraction, the interlayer spacing of graphite and GO can be determined using the Equation (2):

$$N\lambda = 2d\sin\theta \tag{2}$$

where λ, N, and d represent the wavelength of X-ray, diffraction order, and interlayer distance, respectively. The value of interlayer distancing of GO is d_{002} = 8.71 Å, while for natural graphite, this value is d_{002} = 3.35 Å. In other words, the interlayer distancing in the case of GO is almost twice as in natural graphite, which consequently facilitates the penetration of polymer chains between nanosheets. For flax/epoxy composites, the peaks that appeared in 2θ = 15.5, 16.5, and 22.8° are attributed to (1 0 $\bar{1}$), (0 0 2), and (004) reflections of cellulose [22]. It should be mentioned

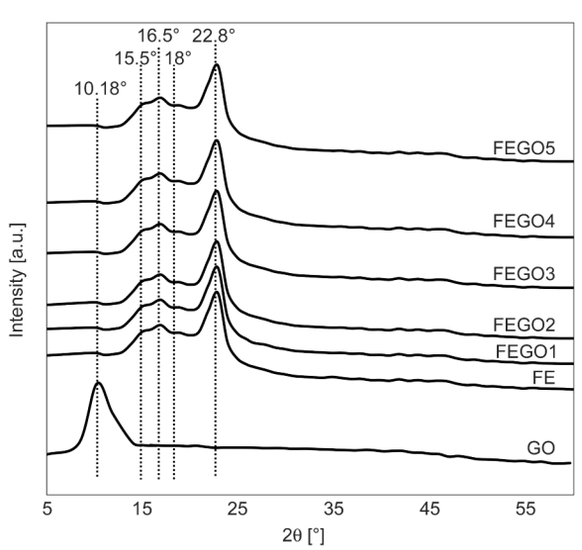

Figure 3. XRD spectra of GNPs, pure epoxy, plain flax/epoxy, and its nanocomposites.

that the peak pertaining to epoxy, because of lower intensities, is not distinguishable in XRD spectra of flax/epoxy composites. Generally, any alteration in intensity or position or peak pertaining to GO can provide worthwhile information about intercalation or exfoliation in the resulting nanocomposites. The disappearance of GO peaks in XRD can be ascribed to the degree of exfoliation in the matrix [23, 24]. As observed, the diffraction peak at 2θ = 10.18° completely disappears in flax/epoxy/GO nanocomposites, exemplifying the formation of an exfoliated structure. While in GNPs reinforced flax/epoxy composites, it is almost next to impossible to achieve an exfoliated structure [12], in flax/epoxy/GO, thanks to the functional groups of GO, the formation of this structure is obtainable, which then is expected to maximize the performance of final nanocomposites against different loads.

3.2.2. Transmission electron microscopy (TEM)

In order to observe the dispersion and the network structure of GO in flax/epoxy nanocomposites, TEM images of samples were captured and shown in Figure 4. As discussed earlier, nanoparticles with high aspect ratio, such as GNPs and GO, because of van der Waals forces tend to stack to each other and form agglomerations which will become stress concentration points once a load is applied to the nanocomposite. As seen, GO has an exfoliated structure in all nanocomposites and no agglomeration is witnessed (as indicated by yellow arrows). Compared to GNPs, the existence of oxygen functional groups on the surface of GO heightens its compatibility with epoxy matrix, which facilitates the exfoliation of nanoparticles [23–25]. Moreover, these functional groups increase the interaction between matrix and nanoparticles, which will efficaciously heighten the

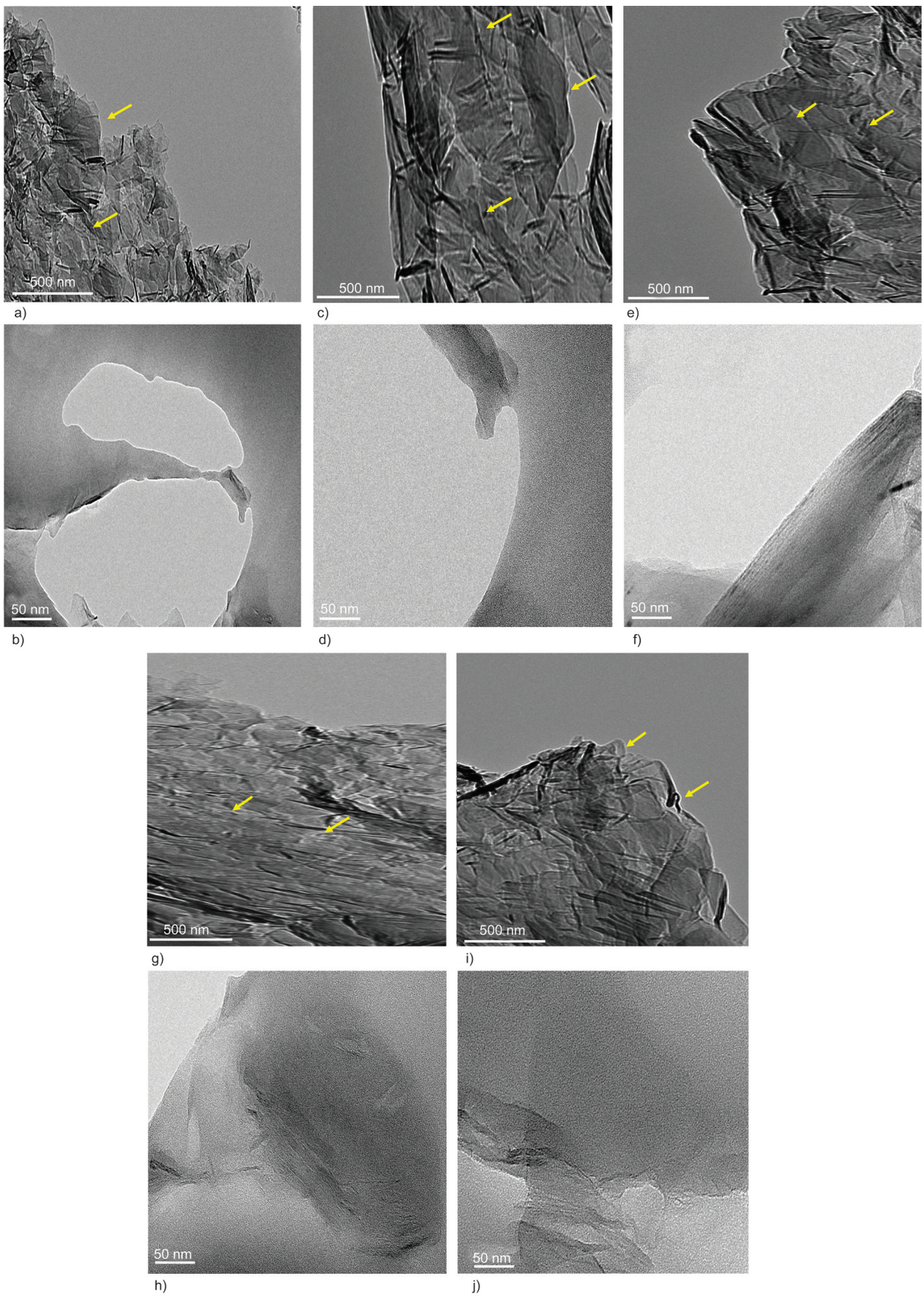

Figure 4. TEM images of flax/epoxy nanocomposites a), b) FEGO1, c), d) FEGO2, e), f) FEGO3, g), h) FEGO4 and i), j) FEGO5.

load-carrying capability of nanocomposites [24]. Therefore, consistent with XRD results, in all GO loadings, an exfoliated structure has formed that is expected to enhance the mechanical properties of nanocomposites.

3.3. Calculation of crosslink density

The values of crosslink density in flax/epoxy/GO nanocomposites were determined using DMA results, Figure 5, with the aid of the elastic modulus above the glass transition temperature by using the rubber elasticity theory according to the Equation (3):

$$\delta = \frac{G}{RT} \tag{3}$$

where δ represents the crosslink density, G is the storage modulus in the rubbery region well above the glass transition temperature, R is the universal gas constant, and T is the temperature at which the storage modulus was selected. As Figure 5 shows, the crosslink density increases up to 0.3 wt% of GO, and from this content onward, it starts to decrease. This issue is rooted in the participation of GO in the curing reaction between epoxy and amine curing agents [13].

3.4. Mechanical properties

The mechanical properties of flax/epoxy composites reinforced with different contents of GO are shown in Table 1. As seen, tensile and flexural properties show an upward trend with the addition of GO and reach the highest point at 0.3 wt% of GO, corresponding to a maximum improvement of 68, 38, 65, 34%, respectively, in tensile strength, Young's modulus, flexural strength and flexural modulus in comparison with FE composite. Incorporation of GO substantially improves the tensile and flexural strength of composites because the interfacial bonding between epoxy matrix and flax fiber is stronger with the presence of GO. As a result, the capability of load transfer from matrix to fiber will improve, inducing nanocomposites to resist a higher load [13]. Generally, a strong interfacial adhesion and consequently a high load-carrying capability are vital for composites to withstand the applied stress. Once composites are exposed to a mechanical force, the polymer matrix will transfer the load to the nanoparticles, and they will carry the majority of the load. The higher interfacial strength efficiently enhances the capability of composites and thus heightens the mechanical strength of composites [13]. Generally, the improvement in GO-incorporated composites is ascribed to several factors, including high strength and Young's modulus of GO, better interaction between polymer matrix/GO, and also the formation of an exfoliated structure thanks to the functional groups on the surface of GO [13, 24, 26]. GO contains oxygen groups that establish bonds with epoxy. Additionally, oxygen functionalization and the small thickness of GO will create a wrinkled and rough surface in nanosheets. Thus, from one side, wrinkled sheets will create mechanical interlocking with the polymer matrix, and from the other side, the chemical reaction between functional groups on the surface of GO and epoxy will contribute to the formation of strong interfacial interactions and adhesion, eventually leading to improved load transfer capability of nanocomposites [13, 22, 26]. The bond created between epoxy and GO and fiber is responsible for stress distribution because when the composite is exposed to the load, the polymer matrix, thanks to its low modulus, is the first point in which the crack initiates.

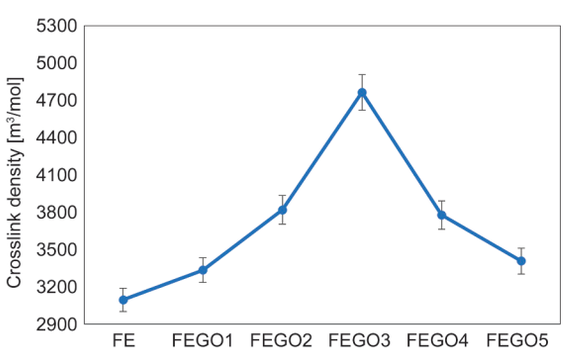

Figure 5. Crosslink density of flax/epoxy nanocomposites.

Table 1. Mechanical properties of the flax/epoxy/GO nanocomposites.

Sample ID	Tensile strength [MPa]	Tensile modulus [GPa]	Flexural strength [MPa]	Flexural modulus [GPa]	Interlaminar shear strength [MPa]
FE	72.5±0.3	4.95±0.07	122.1±1.3	5.30±0.04	14.3±0.3
FEGO1	90.6±0.2	5.49±0.06	167.1±2.9	5.78±0.01	16.2±0.2
FEGO2	102.9±0.3	6.20±0.04	181.7±1.9	6.50±0.02	17.4±0.1
FEGO3	121.8±0.4	6.83±0.05	201.3±3.2	7.10±0.03	18.8±0.4
FEGO4	108.7±0.2	6.50±0.02	173.1±1.6	6.90±0.02	18.1±0.1
FEGO5	101.5±0.1	6.40±0.04	168.2±2.6	6.66±0.04	17.8±0.2

Besides, the mechanical properties in fiber-reinforced composites highly depend on the interfacial interactions between fiber and matrix. In this regard, interlaminar shear strength (ILSS) is considered as one of the reliable measurements to find out the efficiency of interfacial interactions [13]. Table 1 clarifies that ILSS in hybrid composites increases by the incorporation of GO. An increase of 32% is observed in ILSS is noticed in nanocomposite FEGO3. The improvement in ILSS is attributed to the fact that GO possesses oxygen functional groups on its surface, which induce polarity on both surface and the edge of GO which subsequently exert efficacious bonding between the epoxy matrix and GO [13]. Moreover, hydroxyl and epoxy groups on the surface of bisphenol A epoxy resin involve hydrogen bonding between GO molecules, epoxy, and flax fiber. Subsequently, strong interfacial adhesion between epoxy and fiber creates interlocking between composite constituents [13, 22]. This issue is also a result of the wrinkled structure of GO, which brings about the mechanical interlocking between the epoxy matrix and GO [13, 22].

The formation of an exfoliated structure in the epoxy matrix results in more confinement of polymer chains and thus better interaction with nanoparticles. As a result, GO sheets may act as bridging points, enhance the load-carrying ability and thereby the mechanical properties. On the other hand, once the content of nanoparticles exceeds a specific amount, the existence of agglomeration sites then results in the formation of big clusters leading to a decline in the load-carrying capacity of composites. Indeed, when the content of GO is higher than the optimum content, nanoparticles may not separate from each other and thus form agglomeration spots that will further act as stress concentration points. But, according to XRD and TEM results, all nanocomposites had an exfoliated structure. Nevertheless, further addition of GO did not significantly enhance tensile properties. With an increase in the content of GO from 0.3 wt%, the mechanical properties of composites gradually decreased. This issue is attributed to the participation of GO in the curing reaction where the debris of oxidized surface existing on the surface of GO participates in the curing reaction between epoxy and amine. As a result, GO binds with curing agents and leads to weakness in bonding between epoxy and amine curing agent since less amine molecules remain for bonding with epoxy [13]. The reduced extent of crosslinking between epoxy and amine hardener weakens the interfacial interactions between GO, epoxy matrix, and flax fiber. Consequently, a decrease in the mechanical properties of nanocomposites by further addition of GO above 0.3 wt% is observed.

3.5. Evaluation of interfacial adhesion in flax/epoxy/GO nanocomposites

The tensile-fracture surfaces of plain and GO-incorporated composites were examined by optical microscopy images to evaluate the interface between fiber and matrix in flax/epoxy nanocomposites, Figure 6. The less separation between fiber and matrix is an indication of a developed interface which consequently enhances nanocomposite resistance against failure. On the contrary, the higher rate of matrix/fiber separation in flax/epoxy composites will adversely affect the load-carrying capability and thereby deteriorate mechanical properties. As seen in Figure 6, in FE composite, as indicated by yellow arrows, the weak interface results in decohesion of fiber from matrix and matrix micro-cracks, eventually leading to inferior mechanical properties. It is also notable that some microcracks form in the fiber bundle that gradually reach the fiber/matrix interface at which the strength is not high enough to prevent further propagation (as indicated by red arrows). However, in GO-incorporated nanocomposites, the developed interface between fiber and matrix is quite strong, and no separation is observed. The nanocomposites showed a strong bonding at the interface that efficiently arrests the crack and prevents its further development. These observations substantiate that GO efficiently develops the interface between flax fiber and epoxy composites which then will improve the ultimate resistance of the composite against different mechanical loads. Furthermore, the average lengths of cracks, Figure 7, clarify the significance of GO in reducing cracks in resultant nanocomposites. It is quite evident that not only did crack length decrease in nanocomposites, but also the rate of cracks formed at the interface of fiber and matrix significantly reduced.

It also should be mentioned that the constant reduction in crack length happens in FEGO3 nanocomposite, and from that onward, the crack length shows an upward trend. This issue is consistent with mechanical properties where FEGO4 and FEGO5 nanocomposites showed lower tensile and flexural properties as a result of the undesirable participation of GO in the curing reaction between epoxy and amine.

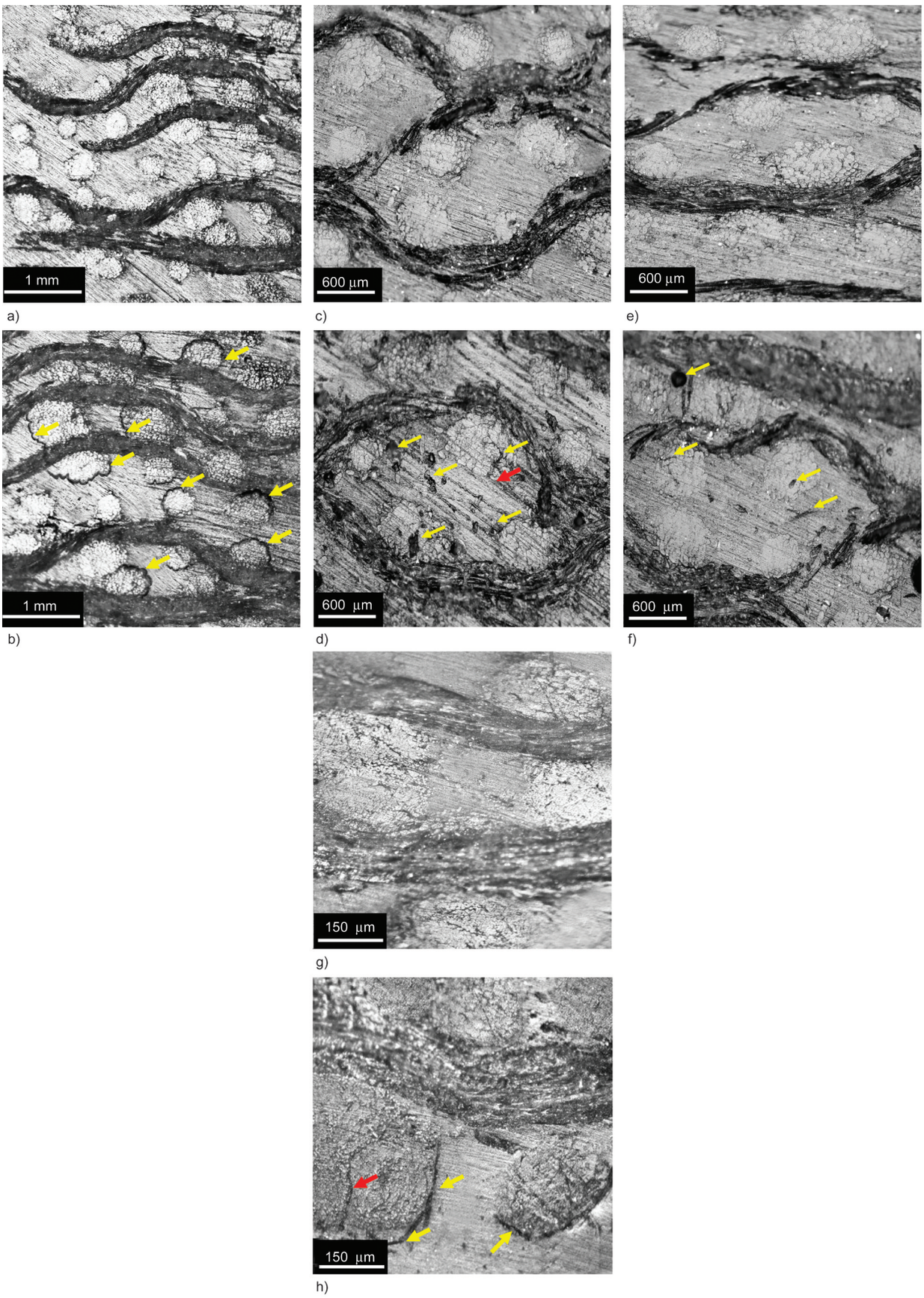

Figure 6. Optical microscopy images captured from the cross section of tensile fracture surface of a), c), e), g) FEGO3 and b), d), f) and h) FE.

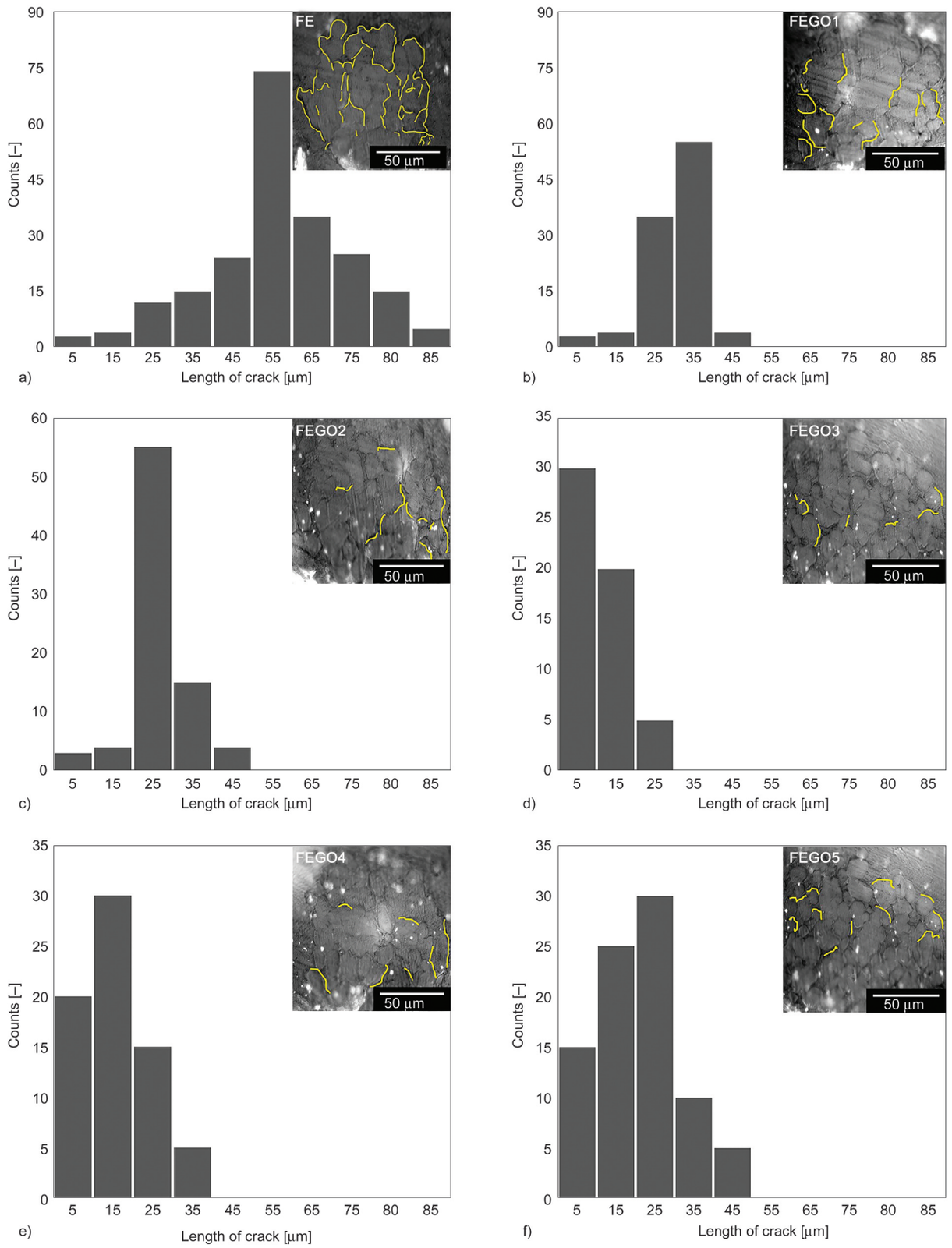

Figure 7. Crack lengths measured for flax/epoxy/GO nanocomposites: a) FE, b) FEGO1, c) FEGO2, d) FEGO3, e) FEGO4, f) FEGO5.

3.6. Morphology of tensile-fracture surfaces of flax/epoxy/GO nanocomposites

The fracture surfaces of FEGO3 nanocomposite are shown in Figure 8. It is quite evident that GO sheets are most likely in broken forms on the epoxy surface while the endpoints of sheets are well embedded in the matrix. The embedded GO sheets in the epoxy matrix confirm that the interface between matrix and

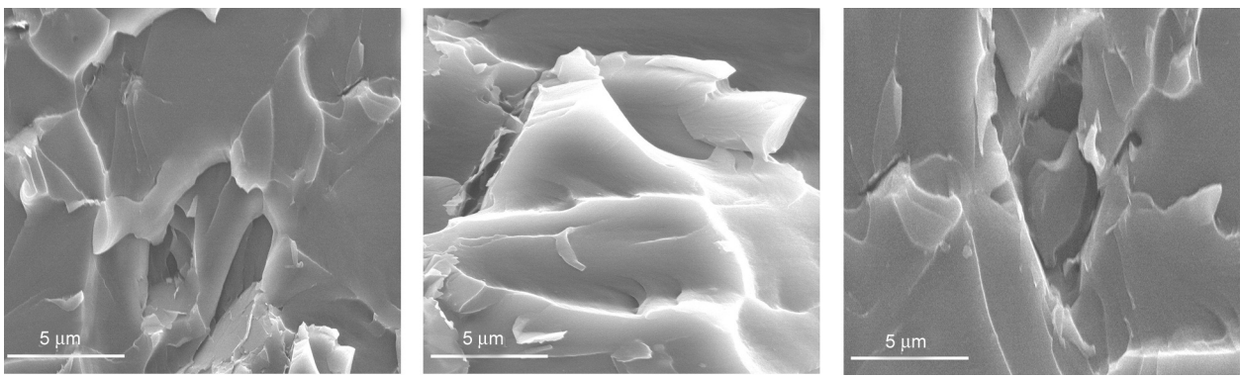

Figure 8. SEM image of fractured surfaces of FEGO3.

nanoparticles is so strong at the time of fracture that complete separation between these two constituents does not happen. The strength of interfacial bonding is attributed to two different matters, including first, the strong Π–Π interaction between GO sheets and the epoxy chain after the solution mixing process and the second chemical reaction between functional groups of epoxy and those on GO sheets. Besides, the fractured surfaces of FE and FEGO3 under the tensile loading are shown in Figure 9. The weak adhesion between matrix and fiber in FE composites results in decohesion of fiber from the matrix. Accordingly, fiber fracture and fiber pull-out are seen in these composites. On the other hand, in FEGO3 nanocomposite, the interfacial interaction between epoxy matrix and flax fiber with the addition of GO increases which leads to higher interaction at the interface of the composite and consequently improves load-carrying capacity. The presence of nanocomposite matrix residual on the surface of flax fiber is seen in Figures 10b and 10d exemplifies the stronger and more developed interface between flax fiber and epoxy matrix because of the higher affinity between fiber and matrix [25]. In FE composites, Figures 10a and 10c, fiber pull-out and fracture are observed while the surface of the fiber is clean, and the residual epoxy is not discerned on the surface of the flax fiber. This issue shows that the interfacial strength between

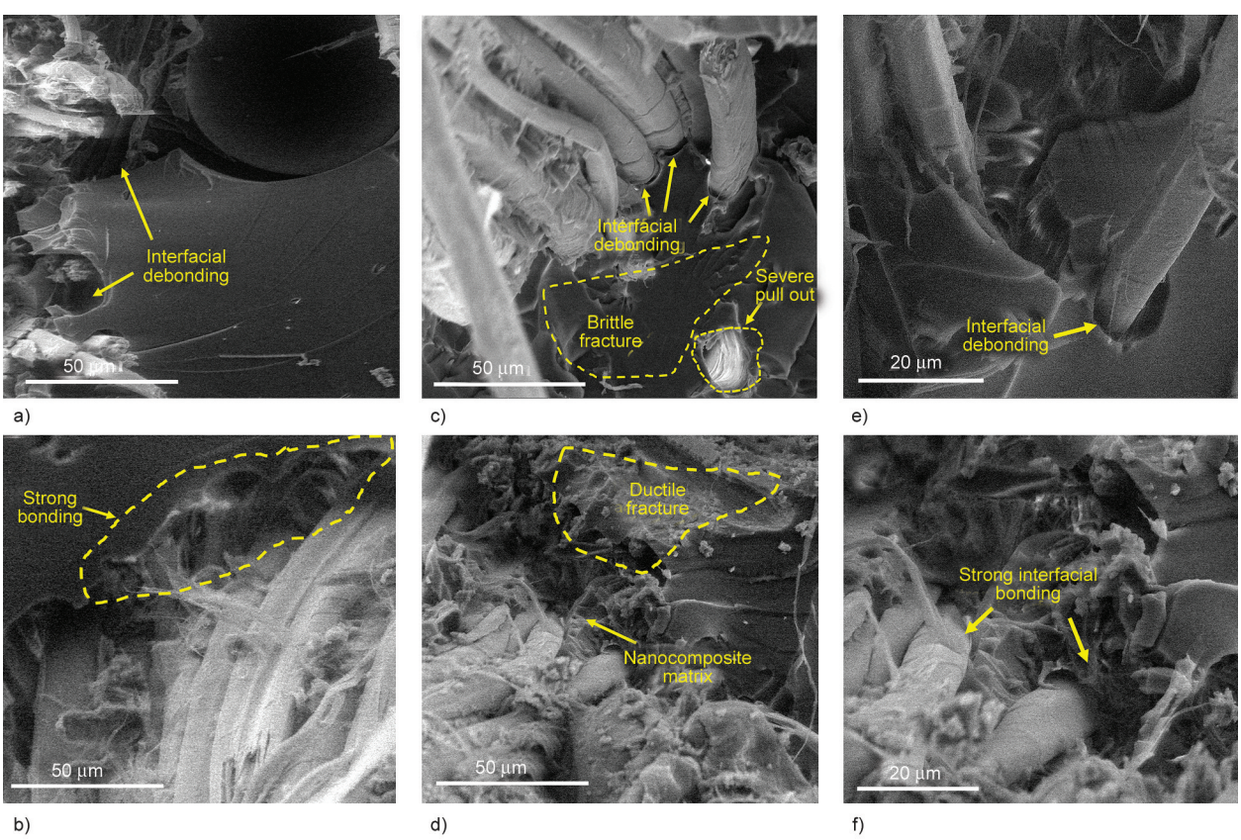

Figure 9. SEM image of fractured surfaces of a), c), e) FE and b), d), f) FEGO3.

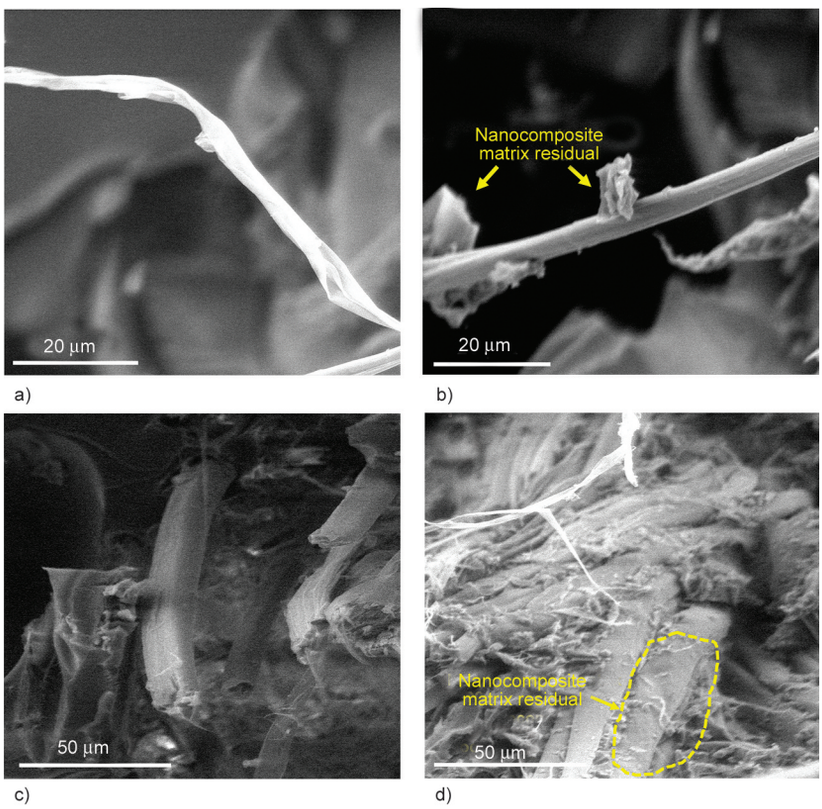

Figure 10. SEM image of fractured surfaces of a), c) FE and, b), d) FEGO3.

fiber and matrix is weak, and expectedly, matrix load-carrying capability is quite low. As discussed earlier, the epoxy and hydroxyl groups existing in epoxy resin create a hydrogen bond with GO molecules. Besides, the creation of interlocking between epoxy chains and GO molecules also results in increased adhesion between fiber and matrix [24]. GO sheets have a high surface area that is hypothesized to induce an exfoliated structure in the matrix and thereby improve the adhesion between fiber and matrix [27]. Once the load is applied to the composite, it will be transferred from the matrix to the fiber, and at this stage, two-dimensional GO sheets are twisted and help the composite absorb much more energy which is responsible for crack development. The twisting behavior of GO sheets, along with the chemical bonding with the polymer matrix, constrain the mobility of epoxy chains in the composite [24].

3.7. Low-velocity impact properties of flax/epoxy/GO manocomposites

The effects of the developed interface between fiber and matrix, due to GO incorporation, on low-velocity impact properties of flax/epoxy nanocomposites were investigated, and the results are shown in Figure 11. For a better comparison, the critical parameters of the curve were extracted and summarised in Table 2. The typical force-displacement curve can be divided into disparate sections. First, the composite sample undergoes the applied load until the maximum point of the curve. The response of the sample in this region is a purely elastic response pertaining to damage initiation energy, which is used by the laminate to rebound from the impactor. Indeed, damage initiation energy in the force-displacement curve is defined as the point at which the maximum load occurs. As observed in Table 2, compared to FE composite, crack initiation energy increases in nanocomposite samples. After this point, the energy absorbed by the composite laminate, known as crack propagation energy, contributes to the creation of damage in the forms of delamination and fiber breakage. Therefore, the larger this area would be, the more severe damage the composite laminate will undergo. In this regard, as observed in Figure 11 and Table 2, the addition of GO up to 0.3 wt% dramatically decreases the amount of absorbed energy by the laminate, indicating higher resistance against the applied load. The total absorbed energy by the composite laminate is comprised of damage initiation energy and damage propagation energy. Thus, it can be deduced that GO incorporation develops the interfacial strength

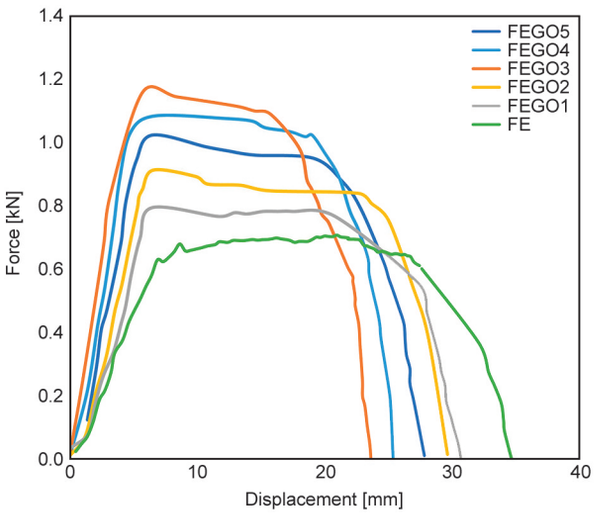

Figure 11. Force-displacement curve of flax/epoxy/GO nanocomposites.

Table 2. Drop weight impact properties of flax/epoxy/GO nanocomposites.

Sample ID	Force [kN]	Crack initiation energy [J]	Crack propagation energy [J]
FE	0.71±0.20	3.80±0.12	15.10±0.3
FEGO1	0.80±0.10	4.40±0.15	14.10±0.7
FEGO2	0.91±0.30	4.90±0.11	13.88±0.5
FEGO3	1.19±0.10	6.10±0.09	11.90±0.3
FEGO4	1.08±0.20	5.70±0.15	12.30±0.4
FEGO5	1.01±0.10	5.40±0.10	12.70±0.4

between fiber and matrix, leading to higher failure initiation energy. It is expected that a weak interfacial adhesion between fiber and matrix contributes to a low peak force and damage initiation energy since low peak force exemplifies the initiation of failure in composites consisting of matrix micro-cracking and interfacial debonding between fiber and matrix, which both are overwhelmingly influenced by fiber/matrix interfacial adhesion [13]. Besides, damage initiation energy and peak force are correlated to each other since a lower peak force is indicative of lower damage initiation energy. Therefore, it can be inferred that the addition of GO not only increases the maximum load that composites can withstand before failure but also enhances the threshold of damage initiation energy. During crack propagation, the energy is absorbed by the laminate through different mechanisms such as fiber breakage, fiber pull-out, delamination, and debonding. The overwhelming part of the impact energy is absorbed in the propagation stage rather than the initiation stage. FE composite shows higher amount of crack propagation energy and low peak force due to poor resistance leading to high absorption energy in the form of delamination and plastic deformation. Consistent with the discussed results, a significant reduction in the value of displacement with the addition of GO is also observed. The reduced displacement indicates the higher ability of the nanocomposite to resist delamination when the impact energy is absorbed by the composite. The higher peak force and lower displacement suggest a higher modulus and damage tolerance in nanocomposites [28, 29].

Figures 12 and 13 show SEM images of the impact-fractured surface of flax/epoxy nanocomposites. As seen, the weak interfacial adhesion between flax fiber and epoxy matrix in FE composites, Figure 12, results in different fracture mechanisms while exposed to the impact force. Fiber fracture (Figure 12a), matrix fracture (Figure 12b), fiber pull out (Figure 12c), and fiber/matrix separation (Figure 12d) are observed as the dominant mechanisms responsible for the dissipation of applied impact energy [28]. Additionally, as observed in Figure 13, fiber/matrix debonding (Figure 13a) and fiber breakage (Figure 13c) substantially happen in FE composites once the laminate is exposed to the impact force. On the contrary, in FEGO3 nanocomposites (Figures 13b and 13d) the strong bonding between flax fiber and the epoxy matrix is observed, that consequently enhances the laminate resistance against the impact force. These observations are consistent with data pertaining to force-displacement curves where FEGO3 nanocomposite, compared to FE composites, showed higher crack initiation energy and lower crack propagation energy thanks to strong bonding between matrix and fiber in the presence of GO.

4. Conclusions

In this study, flax/epoxy composites were reinforced with GO to develop the interface between fiber and matrix by creating an efficient bonding. The FTIR results indicated that the functional groups on the surface of GO led to the creation of bonding between composite constituents that further enhanced the composite tolerance against mechanical loads. Microstructure observations clarified that flax/epoxy nanocomposites achieved an exfoliated structure. The diffraction peak pertaining to GO in XRD spectra of nanocomposites disappeared which is an indication of this structure. These finding were also substantiated by TEM images showing an exfoliated structure of nanoparticles in flax/epoxy/GO nanocomposites.

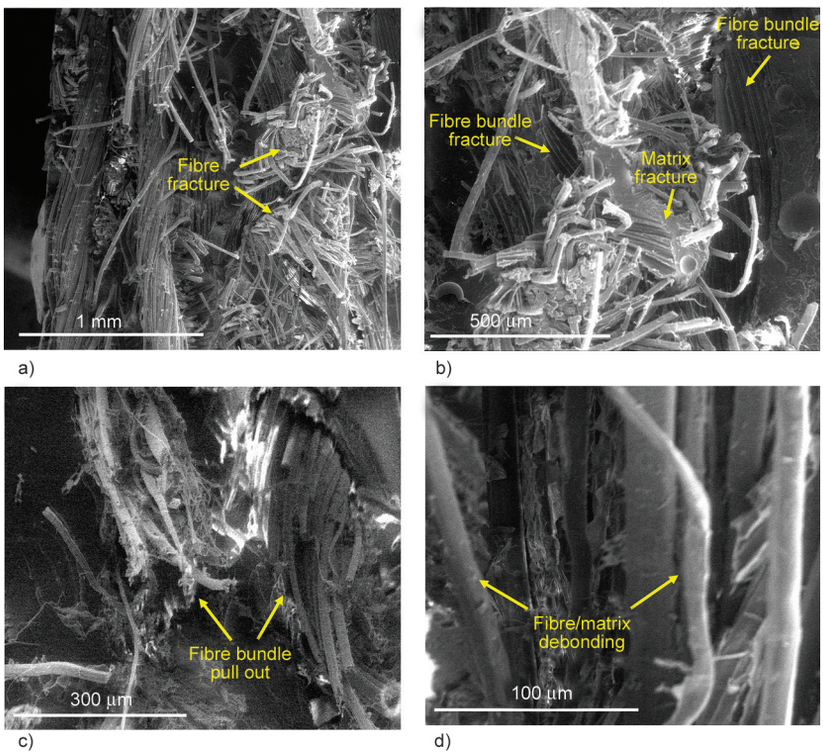

Figure 12. SEM micrographs of impact fracture surface of FE indicating different fracture mechanisms: a) fiber fracture, b) matrix fracture, c) fiber bundle pull out, d) fiber/matrix debonding.

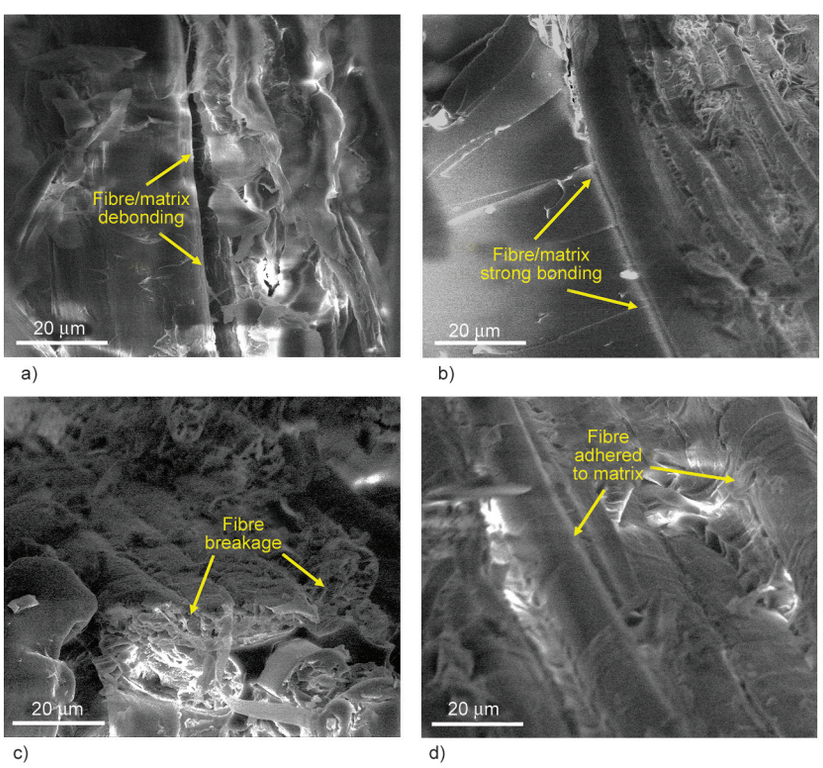

Figure 13. SEM micrographs of impact fracture surface of a), c) FE and b), d) FEGO3.

Mechanical properties of nanocomposites increased significantly up to 0.3 wt% of GO. Beyond this content, due to the participation of GO in the curing reaction between epoxy and hardener, the reinforcing efficiency decreased. SEM and optical microscopy examinations showed that while unreinforced flax/epoxy composites had a weak interfacial adhesion, GO addition strengthened the interfacial adhesion between fiber and matrix and consequently reduced created cracks. Low-velocity impact analysis showed

that GO successfully enhanced damage propagation energy in flax/epoxy composites, which resulted in a reduction in crack propagation energy and less severe damage in nanocomposites.

References

[1] Duc F., Bourban P. E., Plummer C. J. G., Månson J-A. M.: Damping of thermoset and thermoplastic flax fibre composites. Composites Part A: Applied Science and Manufacturing, **64**, 115–123 (2014). https://doi.org/10.1016/j.compositesa.2014.04.016

[2] Bourmaud A., Beaugrand J., Shah D. U., Placet V., Baley C.: Towards the design of high-performance plant fibre composites. Progress in Materials Science, **97**, 347–408 (2018). https://doi.org/10.1016/j.pmatsci.2018.05.005

[3] Joshi S. V., Drzal L. T., Mohanty A. K., Arora S.: Are natural fiber composites environmentally superior to glass fiber reinforced composites? Composites Part A: Applied Science and Manufacturing, **35**, 371–376 (2004). https://doi.org/10.1016/j.compositesa.2003.09.016

[4] Islam M. S., Pickering K. L., Foreman N. J.: Influence of alkali fiber treatment and fiber processing on the mechanical properties of hemp/epoxy composites. Journal of Applied Polymer Science, **119**, 3696–3707 (2011). https://doi.org/10.1002/app.31335

[5] Coroller G., Lefeuvre A., le Duigou A., Bourmaud A., Ausias G., Gaudry T., Baley C.: Effect of flax fibres individualisation on tensile failure of flax/epoxy unidirectional composite. Composites Part A: Applied Science and Manufacturing, **51**, 62–70 (2013). https://doi.org/10.1016/j.compositesa.2013.03.018

[6] Merotte J., le Duigou A., Kervoelen A., Bourmaud A., Behlouli K., Sire O., Baley C.: Flax and hemp nonwoven composites: The contribution of interfacial bonding to improving tensile properties. Polymer Testing, **66**, 303–311 (2018). https://doi.org/10.1016/j.polymertesting.2018.01.019

[7] Marrot L., Bourmaud A., Bono P., Baley C.: Multi-scale study of the adhesion between flax fibers and biobased thermoset matrices. Materials and Design, **62**, 47–56 (2014). https://doi.org/10.1016/j.matdes.2014.04.087

[8] Fernández J. A., le Moigne N., Caro-Bretelle A. S., el Hage R., le Duc A., Lozachmeur M., Bono P., Bergeret A.: Role of flax cell wall components on the microstructure and transverse mechanical behaviour of flax fabrics reinforced epoxy biocomposites. Industrial Crops and Products, **85**, 93–108 (2016). https://doi.org/10.1016/j.indcrop.2016.02.047

[9] Acar V., Erden S., Sarıkanat M., Seki Y., Akbulut H. Seydibeyoğlu M.: Graphene oxide modified carbon fiber prepregs: A mechanical comparison of the effects of oxidation methods. Express Polymer Letters, **14**, 1106–1115 (2020). https://doi.org/10.3144/expresspolymlett.2020.90

[10] Seghini M. C., Touchard F., Sarasini F., Chocinski-Arnault L., Tirillò J., Bracciale M. P., Zvonek M., Cech V.: Effects of oxygen and tetravinylsilane plasma treatments on mechanical and interfacial properties of flax yarns in thermoset matrix composites. Cellulose, **27**, 511–530 (2020). https://doi.org/10.1007/s10570-019-02785-3

[11] Zhang X. Q., Hu G. L., Cen L., Lei C. H.: Enhancing interfacial properties of carbon fiber/polyamide 6 composites by *in-situ* growing polyphosphazene nanotubes. Express Polymer Letters, **15**, 878–886 (2021). https://doi.org/10.3144/expresspolymlett.2021.70

[12] Alipour A., Lin R., Jayaraman K.: Effects of graphene network formation on microstructure and mechanical properties of flax/epoxy nanocomposites. Journal of Materials Research and Technology, **15**, 4610–4622 (2021). https://doi.org/10.1016/j.jmrt.2021.10.082

[13] Pathak A. K., Borah M., Gupta A., Yokozeki T., Dhakate S. R.: Improved mechanical properties of carbon fiber/graphene oxide-epoxy hybrid composites. Composites Science and Technology, **135**, 28–38 (2016). https://doi.org/10.1016/j.compscitech.2016.09.007

[14] Hasan K. M., Horváth P. G., Alpár T.: Potential natural fiber polymeric nanobiocomposites: A review. Polymers, **12**, 1072 (2020). https://doi.org/10.3390/polym12051072

[15] da Luz F. S., da Costa Garcia Filho F., del-Rio M. T. G., Nascimento L. F. C., Pinheiro W. A., Monteiro S. N.: Graphene-incorporated natural fiber polymer composites: A first overview. Polymers, **12**, 1601 (2020). https://doi.org/10.3390/polym12071601

[16] Hummers W. S., Offeman R. E.: Preparation of graphitic oxide. American Chemical Society, **80**, 1339 (1958). https://doi.org/10.1021/ja01539a017

[17] Haghnegahdar M.: Evaluation of specific total work of fracture in polypropylene/ethylene-propylene diene monomer nanocomposites based on various graphene derivatives: Optimization by response surface methodology technique and correlation with microstructure properties. Polymer Composites, in press (2022). https://doi.org/10.1002/pc.27131

[18] Ma Y., Zhao Y., Li F., Xu Y., Wei X., Chen Y., Wang J., Jin H.: Influence of graphene oxide content on the morphology and properties of carbon fiber/epoxy composites. Polymer Composites, **42**, 5574–5585 (2021). https://doi.org/10.1002/pc.26248

[19] Sarker F., Karim N., Afroj S., Koncherry V., Novoselov K. S., Potluri P.: High-performance graphene-based natural fiber composites. ACS Applied Materials and Interfaces, **10**, 34502–34512 (2018). https://doi.org/10.1021/acsami.8b13018

[20] Pereira A. C., Monteiro S. N., Simonassi N. T., Vieira C. M. F., Lima A. M., Costa U. O., Pinheiro W. A., Oliveira M. S., da Silva Figueiredo A. B.: Enhancement of impact toughness using graphene oxide in epoxy composite reinforced with ramie fabric. Composite Structures, **282**, 115023 (2022). https://doi.org/10.1016/j.compstruct.2021.115023

[21] Mohan V. B., Jakisch L., Jayaraman K., Bhattacharyya D.: Role of chemical functional groups on thermal and electrical properties of various graphene oxide derivatives: A comparative X-ray photoelectron spectroscopy analysis. Materials Research Express, **5**, 035604 (2018). https://doi.org/10.1088/2053-1591/aab316

[22] Huner U.: Effect of chemical surface treatment on flax-reinforced epoxy composite. Journal of Natural Fibers, **15**, 808–821 (2018). https://doi.org/10.1080/15440478.2017.1369207

[23] Zaman I., Kuan H-C., Meng Q., Michelmore A., Kawashima N., Pitt T., Zhang L., Gouda S., Luong L., Ma J.: A facile approach to chemically modified graphene and its polymer nanocomposites. Advanced Functional Materials, **22**, 2735–2743 (2012). https://doi.org/10.1002/adfm.201103041

[24] Kooshki M. M., Jalali-Arani A.: High performance graphene oxide/epoxy nanocomposites fabricated through the solvent exchange method. Polymer Composites, **39**, E2497–E2505 (2018). https://doi.org/10.1002/pc.24803

[25] Hou W., Gao Y., Wang J., Blackwood D. J., Teo S.: Recent advances and future perspectives for graphene oxide reinforced epoxy resins. Materials Today Communications, **23**, 100883 (2020). https://doi.org/10.1016/j.mtcomm.2019.100883

[26] Adak N. C., Chhetri S., Kim N. H., Murmu N. C., Samanta P., Kuila T.: Static and dynamic mechanical properties of graphene oxide-incorporated woven carbon fiber/epoxy composite. Journal of Materials Engineering and Performance, **27**, 1138–1147 (2018). https://doi.org/10.1007/s11665-018-3201-5

[27] Javanshour F., Ramakrishnan K. R., Layek R. K., Laurikainen P., Prapavesis A., Kanerva M., Kallio P., van Vuure A. W., Sarlin E.: Effect of graphene oxide surface treatment on the interfacial adhesion and the tensile performance of flax epoxy composites. Composites Part A: Applied Science and Manufacturing, **142**, 106270 (2021). https://doi.org/10.1016/j.compositesa.2020.106270

[28] de Paiva J. M. F., Frollini E.: Unmodified and modified surface sisal fibers as reinforcement of phenolic and lignophenolic matrices composites: Thermal analyses of fibers and composites. Macromolecular Materials and Engineering, **291**, 405–417 (2006). https://doi.org/10.1002/mame.200500334

[29] Safamanesh A., Mousavi M., Khosravi H., Tohidlou E.: On the low-velocity and high-velocity impact behaviors of aramid fiber/epoxy composites containing modified-graphene oxide. Polymer Composites, **42**, 608–617 (2021). https://doi.org/10.1002/pc.25851